ISBN: 978-3-95450-201-1 doi:10.18429/JACoW-IBIC2018-WEOC04

SPACE CHARGE EFFECTS STUDIES FOR THE ESS COLD LINAC BEAM PROFILER

F. Belloni†, F. Benedetti, J. Marroncle, P. Abbon, G. Coulloux, F. Gougnaud, C. Lahonde-Hamdoun, P. Le Bourlout, Y. Mariette, J. P. Mols, V. Nadot, L. Scola,
CEA-Saclay, 91191 Gif-sur-Yvette, France
C. Thomas, ESS, 221 00 Lund, Sweden

Abstract

Five Ionisation Profile Monitors are being built by CEA in the framework of the in-kind contribution agreement signed with ESS. The IPMs will be installed in the Cold Linac where the proton energy range they need to cover extends from 90 MeV to 2 GeV. The ESS fields intensity of 1.1e+09 protons/bunch delivered at a frequency of 352 or 704 MHz, with a duty cycle of 4%, may strongly affect the trajectories of the ionised molecules and electrons created by the passage of the beam through the residual gas. In order to quantify and to develop a correction algorithm for these space charge effects, a code was initiated at ESS and completed at CEA Saclay with the possibility to include real case electric fields calculated with Comsol Multiphysics. A general overview of the code and its preliminary results are presented here.

INTRODUCTION

The first proton beam at the European Spallation Source (ESS), in construction at Lund (Sweden) is expected by 2019. A perfect beam alignment and focusing are necessary to prevent beam losses and the resulting activation of the accelerator and pipes. Transversal beam profile monitors are therefore among the diagnostics needed by the accelerator.

ESS proton fields are too intense for interceptive monitors, causing material vaporization and radiation damage. Non invasive monitors are the only option for monitoring the ESS transversal beam profile. NPMs (Non-Interceptive Profile Monitors) can rely on ionisation (IPMs) or on fluorescence emission (FPMs). The two processes have different cross sections at different energies, the latter being less likely at high proton energies than the former.

The Cold Linac, where the pressure is expected to be below 10^{-9} mbar, will be therefore equipped with 5 NPMs of IPM type: one in the Spoke section (protons in the 90 MeV - 216 MeV energy range), 3 in the Medium β section (216 MeV – 571 MeV) and one in the High β section (571 MeV – 2 GeV). Every NPM will be installed in a chamber in-between the cryomodules and is composed of two IPMs set at 90° with respect to each other, and each one measuring one transversal beam profile.

Physically, an ESS-IPM is a cube missing two opposite walls. Out of the four remaining walls, two opposite ones are metallized to be used as electrodes for imposing an electric field in the cage and the other two are in insulating material but equipped with resistors to make the field as more uniform as possible. The proton beam enters the cage through one missing wall and exits from the other missing one.

SPACE CHARGE EFFECTS

The effects of space charge are twofold: they affect the charged particle beam itself and any other charge in its proximity. Our focus is on this second aspect.

A charge generated at rest between two parallel plates kept at different voltages drifts towards the electrodes travelling parallel to the electric field lines. In an ideal case of perfectly uniform electric field, the point where the charge meets the plate will simply be the projection of its initial position on the electrode. In IPMs, charges are created via gas ionisation and the beam profile is reconstructed this way. But the presence of a charged particle beam, necessary to create ionisation charges, induces an electromagnetic field which modifies the trajectories of the electrons and of the ionised gas molecules and thus introduces a shift between the point where they should have ideally meet the electrode and the point where they really reach it. The measured beam profile therefore will differ from the real one by an amount which depends on the beam intensity, the beam size, the beam energy and the strength of the electric field applied between the electrodes.

CODE TO QUANTIFY THE SPACE CHARGE EFFECTS

ESS Core

The core of the code was written in MATLAB at ESS [1] and translated in C++ at CEA Saclay. Its mathematics is based on [2]. Briefly, let's consider the reference frames K and K, with cartesian axis respectively x,y,z and x,y and z. K is the laboratory system where a Gaussian bunch with total charge Q_b is moving with speed v_b along the z axis, while K is the reference frame co-moving with the bunch. The charge density of the bunch in the co-moving frame is given in Eq. (1)

$$\rho(\bar{x},\bar{y},\bar{z}) = \frac{Q_b}{(2\pi)^{3/2}\sigma_{\bar{x}}\sigma_{\bar{y}}\sigma_{\bar{z}}}\exp\left(-\frac{\bar{x}^2}{2\sigma_{\bar{x}}{}^2}\right)\exp\left(-\frac{\bar{y}^2}{2\sigma_{\bar{y}}{}^2}\right)\exp\left(-\frac{\bar{z}^2}{2\sigma_{\bar{z}}{}^2}\right) \quad (1)$$

†francesca.belloni@cea.fr

ISBN: 978-3-95450-201-1 doi:10.18429/JACoW-IBIC2018-WEOC04

The electric potential Φ generated by such charge density can be calculated in the co-moving system from the Poisson equation:

$$\nabla^2\Phi(\bar{x},\bar{y},\bar{z}) = -\frac{1}{\epsilon_0}\rho(\bar{x},\bar{y},\bar{z}) \tag{2}$$

The solution to Eq. (2) results:

$$\Phi(\bar{x},\bar{y},\bar{z}) = \frac{Q_b}{4\pi\epsilon_0\sqrt{\pi}}\int_0^\infty \exp\left(-\frac{\bar{x}^2}{\xi_{\bar{x}}{}^2}-\frac{\bar{y}^2}{\xi_{\bar{y}}{}^2}-\frac{\bar{z}^2}{\xi_{\bar{z}}{}^2}\right)\frac{1}{\sqrt{\xi_{\bar{x}}\xi_{\bar{y}}\xi_{\bar{z}}}}d\xi \tag{3}$$

with $\xi_x = \xi + \sigma^2{}_x$, $\xi_y = \xi + \sigma^2{}_y$, $\xi_z = \xi + \sigma^2{}_z$, and ξ being an integration variable. The electric field generated by the Gaussian bunch in the co-moving system K is then obtained as:

$$\begin{cases}\overline{E_{\bar{x}}} = -\frac{\partial}{\partial x}\Phi(\bar{x}\bar{y}\bar{z}) \\ \overline{E_{\bar{y}}} = -\frac{\partial}{\partial y}\Phi(\bar{x}\bar{y}\bar{z}) \\ \overline{E_{\bar{z}}} = -\frac{\partial}{\partial z}\Phi(\bar{x}\bar{y}\bar{z})\end{cases} \tag{4}$$

The electric field in the co-moving rest frame can be transformed into electric and magnetic fields in the laboratory frame through Lorentz Transformations as shown in Eq. (5):

$$E = \begin{pmatrix}\gamma_b\overline{E_{\bar{x}}} \\ \gamma_b\overline{E_{\bar{y}}} \\ \overline{E_{\bar{z}}}\end{pmatrix} B = \begin{pmatrix}-\gamma_b\beta_b\overline{E_{\bar{y}}}/c \\ -\gamma_b\beta_b\overline{E_{\bar{x}}}/c \\ 0\end{pmatrix} \tag{5}$$

The force felt by a test charge q because of the electric and magnetic fields is computed as:

$$F = q(E + v \times B) \tag{6}$$

with $\mathbf{v} = (0, vb, 0)$. Once the force has been calculated, the equations of motion can be derived and the trajectory of the charge q under the influence of the electromagnetic fields generated by the Gaussian bunch can be simulated.

CEA Implementation

Two main additions to the code have been implemented at CEA to account for electric field inhomogeneities and for the initial momenta of the ionisation products.

The electric field is fed to the code as a list of 3D points and their corresponding 3D field components (Ex, Ey and Ez) after being simulated using Comsol Multiphysics [3]. A header-only library for Nearest Neighbour (NN) search with KD-trees [4] is used to go through the file generated by Comsol and find the location of the points closest to the position of the test charge. The number N of points searched for is decided by the user. The found N 6D arrays (3D points and 3D fields) are then used as a 3D-net and the value of the electric field at the position of the test charge is computed via Radial Basis Function interpolation.

The momenta of the electrons generated via ionisation are calculated using Garfield++ [5] and fed to the code in an external file. Garfield++ is a toolkit for detailed simulations of particle detectors that use gas and semi-conductors as sensitive medium. Its validity is limited to high energy incident particles (relativistic and quasi relativistic beams) and it can not give information about ionised gas molecules. To compute their momenta, a simplifying assumption is introduced: the incident beam has not been deviated and therefore, for momentum conservation, the electron and ionised molecule are emitted with opposite momenta:

$$v_e = \frac{m_{ion}}{m_e}v_{ion} \tag{7}$$

RESULTS

ESS requires that the transverse beam profile shall be measured with a maximum total error in the RMS extension of the beam of less than ±10%. In order to determine the conditions fulfilling this requirement, several simulations have been performed.

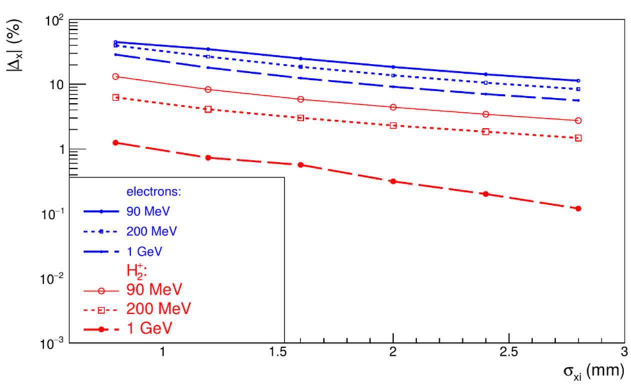

Figure 1: Space charge effects (given as deviation between the beam width input in the simulations and the one obtained by running the code) for different σ_{xi} (i.e. input σ_x) and incident beam energies when σ_y=σ_z= 2mm and **E** = E_y = 300 kV/m.

The residual gas in the accelerator tube at ESS is expected to be composed mainly by hydrogen (79 %) and for this reason the influence of the electromagnetic field generated by the ESS beam on the trajectories of the ionisation products has been performed both for electrons and H_2^+. The space charge effects have been initially computed for different beam energies (90 MeV, 200 MeV and 1 GeV), beam widths (σ_x = 1.2 mm, 1.6 mm, 2 mm, 2.4 mm and 2.8 mm, σ_y = 1.2 mm, 1.6 mm, 2 mm, 2.4 mm and 2.8 mm and σ_z = 2 mm) and uniform electric fields (from 50 kV/m to 300 kV/m). Figure 1 reports the trend of the space charge effects with respect to different σ_x, beam

ISBN: 978-3-95450-201-1 doi:10.18429/JACoW-IBIC2018-WEOC04

energies and test particles when **E** = E_y = 300 kV/m, and both the σ_y and σ_z input in the simulation measure 2 mm.

It is evident that the lower the beam energy and the higher is the deviation between the input beam width and the one obtained by running the code.

This is true for the particular simulations run, but it is not a general rule. As a matter of fact, for a different set of electric field strength and σ_x, σ_y and σ_z values, the opposite behaviour can be obtained. This underlines the complexity of the phenomenon, which results from the interplay of various factors. Nevertheless, it is possible to draw some conclusions. First, the larger the initial beam width and the lower the space charge effects. Finally, the discrepancy between the σ_x input in the simulations and the one obtained as their results is larger for electrons than for ions, due to their high difference in mass.

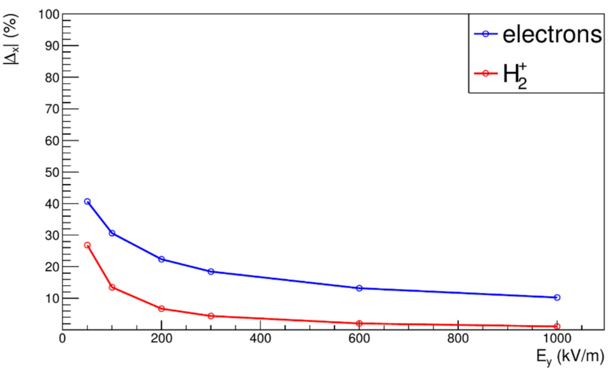

Figure 2: Comparison between the space charge effects for electrons and singly ionised hydrogen molecules H_2^+, for a 90 MeV proton beam with beam size $\sigma_x = \sigma_y = \sigma_z = 2$ mm in an homogeneous electric field.

In Fig. 2 the trend of the space charge effects as a function of a homogeneous electric field **E** = E_y is studied only for lowest possible energy of the cold Linac cryomodule (90 MeV), i.e., for the worst case scenario of the results of Fig. 1. The values of σ_x, σ_y and σ_z were fixed to 2 mm, which corresponds to the average beam size in the Spoke section of the accelerator.

As expected, the lower the field, the lower the speed of the drifting test charges, the more time they spend in the electromagnetic field generated by the ESS beam and the larger the space charge effects.

From Fig. 2 it can be inferred that if electrons are used to measure the beam profile, an electric field higher than 10^6 kV/m is needed to meet the ESS uncertainty requirement of 10%. On the other hand, the same condition is fulfilled for much weaker electric fields if singly ionised hydrogen molecules are detected. A difference of potential of 15 kV between the two electrodes of the IPM cube of 10 cm side is already enough to measure the transverse profile with a maximum total error in the RMS extension of the beam of less than ± 10%. Since these simulations do not account for effects such as the space resolution of the detector and are themselves affected by an uncertainty estimated to less than 2%, it was decided that an electric field higher than 150 kV/m is preferable. As a matter of of fact, to more efficiently counterbalance the space charge effects, the electric field needs to be as high as possible. E_y = 300 kV/m has been selected as maximum electric field realistically reachable in the experimental set-up.

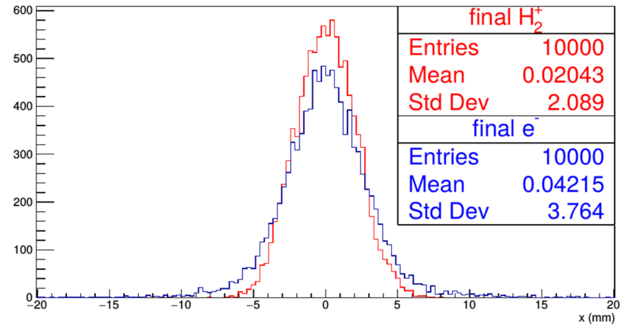

Figure 3: Comparison between the space charge effects felt by electrons and ions when initial momenta distributions are accounted for. Both test charges are created by a 90 MeV proton beam in the Spoke configuration and a perfectly homogeneous electric field **E** = E_y = 300 kV/m has been considered.

The results reported in Fig. 2 are obtained considering that electrons and ions are created at rest. This is not true and the impact of the initial momentum distributions of electrons and H_2^+ on the beam profile measurements has therefore been simulated. The outcome was that this factor is negligible for massive particles, but not for electrons. Figure 3 shows the comparison between the results of the simulations run for the two test charges when the Spoke configuration (90 MeV proton beam with beam size $\sigma_x = \sigma_y = \sigma_z = 2$ mm) and an homogeneous **E** = E_y = 300 kV/m are considered. For these conditions, if electrons are produced at rest, $|\Delta x| < 25\%$, while it increases to $|3.764 - 2|/2 \sim 88\%$ when their initial momenta distributions are accounted for. For singly ionised hydrogen molecules instead $|\Delta x|$ remains stable to ~ 4% both when they are generated at rest and with an initial momentum distribution.

It is therefore evident that, to fulfill the ESS requirement, the IPMs cannot be polarized in such a way to detect electrons on the read-out.

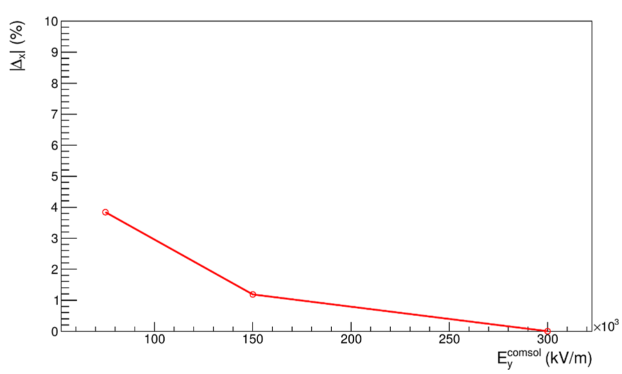

Figure 4: Space charge effects for singly ionised hydrogen molecules H_2^+ created at rest at Spoke conditions for different real case electric fields.

ISBN: 978-3-95450-201-1 doi:10.18429/JACoW-IBIC2018-WEOC04

Finally, real case electric field simulations of two IPMs, orthogonal to each other were performed at CEA-Saclay and fed to the code. This allowed to check the influence of the other field components (E_x and E_z) on the transverse beam profile measurements. Having proved that we can use IPMs only in ion configuration and that, in such a case, the initial momenta distributions can be neglected, a study for H_2^+ molecules created at rest was performed for Spoke conditions and three sets of resistors on the IPMs, giving rise to three different E_y^{COMSOL} field configurations aiming to be as close as possible to $E_y \rightarrow$ 75 kV/m, $E_y \rightarrow$ 150 kV/m and $E_y \rightarrow$ 300 kV/m. Since resistors do not come with every desirable value, a choice towards sets resulting in a slightly focusing electric field was performed at the expenses of sets creating slightly defocusing electric fields. This helps to counterbalance the impact of the space charge effects on the transverse beam profile measurements (see Figure 4).

CONCLUSIONS

Five transversal beam profilers have to be built for the ESS Cold Linac. The nominal gas pressure will be 10^{-9} mbar and it is expected to mainly consist of hydrogen. For this reason, detailed simulations of the space charge effects felt by electrons and H_2^+ molecules have been performed with an in-house code in different steps. In the beginning the ionisation charges were considered to be produced at rest in an ideally homogeneous electric field to study the impact of the beam parameters and of the field itself on their trajectories.

In a second step, the contributions of a real case electric field and of initial momenta distributions of the ionisation products to the misreconstruction of the transversal beam profiler have been separately added to understand their weight.

The studies performed allowed to exclude the possibility of operating the IPMs in electron if the ESS requirement of a maximum total error in the RMS extension of the beam of less than ±10% needs to be fulfilled.

Also, electric fields as high as possible are desirable, keeping always in mind that a top value of 300 kV/m needs to be considered as the highest realistically reachable value in our set-up.

REFERENCES

[1] C.A. Thomas, F. Belloni, and J. Marroncle, “Space charge studies for the ionization profile monitors for the ESS Cold Linac”, in *Proc. 5th Int. Beam Instrumentation Conf. (IBIC’16)*, Barcelona, Spain, Sep. 2016, pp. 555-558. doi:10.18429/JACoW-IBIC16-TUPG81

[2] R. Wanzenberg, “Nonlinear motion of a point charge in the 3D space charge field of a Gaussian bunch”, DESY, Hamburg, Germany, Internal Rep., DESY M 10-01, May 2010.

[3] COMSOL Multiphysics, http://www.comsol.com

[4] nanoflann: a C++11 header-only library for Nearest Neighbor (NN) search with KD-trees, https://github.com/jlblancoc/nanoflann

[5] K. Baraka, S. Biagi, A. Folkestad, J. Renner, H. Schindler, N. Shiell, I. Smirnov, R. Veenhof, and K. Zenker, “Garfield++ simulation of tracking detectors”, http://garfieldpp.web.cern.ch/garfieldpp